

## **AFRREV STECH**

An International Journal of Science and Technology  
Bahir Dar, Ethiopia

Vol. 2 (1) January, 2013: 1-26

ISSN 2225-8612 (Print)

ISSN 2227-5444 (Online)

---

### **2D Flow around a Rectangular Cylinder: A Computational Study**

**Olawore, A.S.**

Department of Mechanical Engineering  
University of Ibadan, Nigeria  
E-mail: olaworesly@yahoo.com

&

**Odesola, I. F.**

Department of Mechanical Engineering  
University of Ibadan, Nigeria  
E-mail: ifodesola@yahoo.com

---

#### **Abstract**

*The unsteady flow around a rectangular cylinder is an area of great research for scientist for several years. A two-dimensional unsteady flow past a rectangular cylinder has been investigated numerically for the low Reynolds numbers (flow is laminar). Gambit has been used throughout this work to generate the geometry and meshes and the computational fluid dynamics analysis is done using fluent software. The influence of vortical structure and pressure distribution around the section of rectangular cylinders are*

*examined and reported. The integral aerodynamic parameters are also reported. Strouhal numbers for Reynolds numbers of 55, 75, 100, 150, 250 and 400 are 0.102, 0.122, 0.129, 0.136, 0.139 and 0.158 respectively. The magnitudes of the coefficient of drag for the Reynolds numbers are 1.565, 1.524, 1.432, 1.423, 1.526 and 1.545. The lift coefficient for flow around a rectangular cylinder with a chord-to-depth ratio equal to 5 of low Reynolds numbers of 55, 75, 100, 150, 250 and 400 are 0.067, 0.101, 0.157, 0.212, 0.404 and 0.537 respectively. The pressure drags obtained in the simulations at zero angle of incidence are 1.446, 1.455, 1.439, 1.412, 1.579 and 1.602 for Reynolds numbers 55, 75, 100, 150, 225, and 250. The velocity across the rectangular cylinders varies from 0.089 to 1.02m/s. The forces caused by vortex shedding phenomenon must be taken into account when designing buildings for safe, effective and economical engineering designs.*

**Key words:** Vortex shedding, laminar, Aerodynamic, Strouhal number, Wake and Von Kármán Street.

### Introduction

Bluff bodies are structures with shapes that significantly disturb the flow around them, as opposed to flow around a streamlined body. Examples of bluff bodies include circular cylinders, square cylinders and rectangular cylinders. Flow around square and rectangular cylinders is a frequent happening in engineering. Tall buildings, monuments, and towers are permanently exposed to wind. Similarly, piers, bridge pillars, and legs of offshore platforms are continuously submitted to the load produced by maritime or fluvial streams. This kind of flow is also found in many other technical applications, especially those concerning with thermal and hydraulic devices (Almeida et al, 2008). The flow around a rectangular cylinder in the uniform flow is the most basic fluid dynamic phenomenon. It is known that the flow around a rectangular cylinder exhibits an unsteady behaviour such as separation flow and reattachment flow, accompanied by a change in fluid dynamic force according to changes in its chord ratio B/D (Okajima, 1990). The study of flow around bluff bodies of rectangular shape has a deep engineering interest because many civil but also industrial structure can be assimilate to this shape. Understanding computational fluid dynamics (CFD) is important in investigating the influences and impacts of fluid flow. This refers particularly to engineering practice, such as the wind effects on tall buildings, chimneys or long span bridges. The fluid-dynamic forces acting on a rectangular cylinder have been mainly investigated for

unbounded flow conditions. In particular from these studies one learns about the flow characteristic around deck sections of long span bridges and tall buildings. These studies are important in terms of aerodynamic design to investigate the structure aerodynamic features in detail (Stefano & Nicola, 2008). Nowadays, the flow around bluff bodies has been widely investigated; the greater numbers of studies concern the flow past circular cylinders. Less attention has been dedicated to the flow around rectangular cylinders, although this phenomenon is of great interest for engineering and aerodynamic applications, especially for the fluid–structure interactions via experimentation and numerical approach. After the first experimental works of Okajima (1982) that investigated the Strouhal number varying the cylinder width-to-height ratio ( $B/D$ ) from 1 to 4 in a wide range of Reynolds numbers, some studies regarding both the laminar and turbulent flows have been performed through numerical and experimental techniques. Okajima (1990) investigated the numerical simulation of flow around a rectangular cylinder at a width-to-height ratio ( $B/D = 1.5$  to 4) on the unsteady 2D flow pattern, at zero angle of incidence at a critical range Reynolds number of flows, whereas Sarioglu et al (2000) carried out experimental and numerical analysis of this phenomenon at moderate Reynolds numbers. Bruno et al. (2008) studied the 3-D flow around a rectangular cylinder at  $Re = 40,000$  by means of a finite volume discretization, whereas Nigro et al. (2005) applied a finite element method to the large eddy simulations of the flow past a sharp-edged surface mounted cube at  $Re = 40,000$ . Rokugou et al. (2002) carried out three-dimensional numerical analysis of the flow around rectangular cylinders with various side ratios,  $D/H$ , from 0.2 to 2.0, for Reynolds number of 1000 by using a multi directional finite difference method on a regular-arranged multi grid. Nakaguchi et al (1968) pointed out that pressure distribution around the cylinder surface provides basic knowledge of the force exerted by the fluid on a body, the pressure distribution varying according to the  $B/H$  ratios of the section.

Numerical modelling in wind engineering is based on methods of computational fluid dynamics (CFD). Coupled with computer aided flow visualization, which provides visual animation, the numerical simulation may serve as a useful tool to analyze the evolution of flow field around structures and the attendant load effects. These techniques are presently in developmental stage and are computationally quite intensive, and like any other modelling procedure; they are not free from error.

All numerical studies rely on a good numerical scheme for the evaluation of the parameters in the sample space. Many numerical methods have been developed over the years which include the finite difference method, finite element method, and spectral method, each with its own advantages and disadvantages. Regardless of the choice of method, the convection term must be properly discretized to insure both accuracy and stability. This makes the computational cost for practical engineering systems with complex geometry or flow configurations, such as turbulent jets, pumps, vehicles, and landing gear, attainable using supercomputers (kai, 2005). The aim of this thesis is to develop proficient and advanced numerical modeling methodology for the simulation of 2D flow around a rectangular cylinder using CFD. In particular, the present paper focuses on three main aspects:

- Firstly, to simulate the flow around a fixed sharp-edged rectangular cylinder with a chord-to-depth ratio equal to 5 at low Reynolds numbers.
- Secondly, to investigate the influence of Reynolds number on quantities such as Strouhal number, lift and drag coefficient.
- Lastly, to investigate the effect of vortical structure and pressure distribution around the sections at low Reynolds numbers.

The Navier-Stokes equations with appropriate boundary conditions are to be approached numerically. The incompressible flow equations are solved using the CFD software package, FLUENT, which is a finite-volume solver. CFD calculates numerical solutions to the equations governing fluid flow. FLUENT shall also be used for solving the Navier-Stokes equations. It contains fundamental components, such as discretization on a staggered grid as well as the visualization of the solution over time. The simulation has to provide 2D, structured meshes, time-dependent geometries, such as local mesh refinement, time step control, time and memory efficiency for large computations.

### **Methodology**

Numerical investigation was performed using commercial software GAMBIT and FLUENT. GAMBIT was used to generate mesh of the flow domain around the rectangular cylinder; these mesh files were then exported in FLUENT to solve the integral aerodynamic parameters. This chapter

describes in detail the numerical technique to solve fluid flow. The conservation of mass and momentum can be written as;

$$\left\{ \begin{array}{l} \frac{D\rho}{Dt} + \rho \frac{\partial u_i}{\partial x_i} = 0 \\ \rho \frac{Du_i}{Dt} = -\frac{\partial p}{\partial x_i} + \frac{\partial \tau_{ij}}{\partial x_j} + \rho F_i \\ \tau_{ij} = \mu \left( \frac{\partial u_i}{\partial x_j} + \frac{\partial u_j}{\partial x_i} - \frac{2}{3} \frac{\partial u_k}{\partial x_k} \delta_{ij} \right) \end{array} \right. \quad (1)$$

For incompressible flow  $\rho = \text{constant}$ , which from the conservation of mass equation implies

$$\frac{\partial u_i}{\partial x_i} = 0 \quad (2)$$

implying that a fluid particle experiences no change in volume. Thus the conservation of mass and momentum reduce to

$$\left\{ \begin{array}{l} \frac{\partial u_i}{\partial t} + u_j \frac{\partial u_i}{\partial x_j} = -\frac{1}{\rho} \frac{\partial p}{\partial x_i} + \nu \nabla^2 u_i + F_i \\ \frac{\partial u_i}{\partial x_i} = 0 \end{array} \right. \quad (3)$$

Where the viscous stress tensor can now be written as

$$\frac{\partial}{\partial x_j} \left( \frac{\partial u_i}{\partial x_j} + \frac{\partial u_j}{\partial x_i} - \frac{2}{3} \frac{\partial u_k}{\partial x_k} \delta_{ij} \right) = \frac{\partial^2 u_i}{\partial x_j \partial x_j} = \nabla^2 u_i \quad (4)$$

$$\nu = \mu / \rho \text{ is the kinematic viscosity (5)}$$

The non-dimensional incompressible Navier-Stokes equation is given as;

$$\begin{cases} \frac{\partial u_i}{\partial t^*} + u_j \frac{\partial u_i}{\partial x_j} = -\frac{\partial p}{\partial x_i} + \frac{1}{\text{Re}} \nabla^2 u_i \\ \frac{\partial u_i}{\partial x_i} = 0 \end{cases} \quad (6)$$

### Flow modelling and computational approach

The domain discretization into control volumes is necessary for the finite volume method used in the FLUENT. This CFD software solves the equations of mass and momentum in each control volume, guarantying conservation for each variable. Flow past a rectangular cylinder has been simulated by solving numerically the unsteady Navier-Stokes equations for an incompressible fluid in a two-dimensional geometry. The equations for continuity and momentum may be expressed in the dimensionless form as follows:

Continuity

$$\frac{\partial u}{\partial x} + \frac{\partial v}{\partial y} = 0 \quad (7a)$$

X-momentum

$$\frac{\partial u}{\partial t} + \frac{\partial}{\partial x}(uu) + \frac{\partial}{\partial y}(vu) = -\frac{\partial p}{\partial x} + \frac{1}{\text{Re}} \left( \frac{\partial^2 u}{\partial x^2} + \frac{\partial^2 u}{\partial y^2} \right) \quad (7b)$$

Y-momentum

$$\frac{\partial v}{\partial t} + \frac{\partial}{\partial x}(uv) + \frac{\partial}{\partial y}(vv) = -\frac{\partial p}{\partial y} + \frac{1}{\text{Re}} \left( \frac{\partial^2 v}{\partial x^2} + \frac{\partial^2 v}{\partial y^2} \right) \quad (7c)$$

### Computational domain, boundary conditions and assumptions

The configuration for the simulation is illustrated in an arbitrary scale in Figure 1. The rectangular cylinder is placed at  $6B$  from the upstream and  $13B$  from the downstream, where  $B$  is the breadth. The cylinder rectangular cross section is characterized by sharp edges and smooth surfaces. The velocity of fluid at the inlet is fixed to the value of  $1\text{m/s}$ . The Reynolds numbers are based on  $U_x$  and  $D$ .

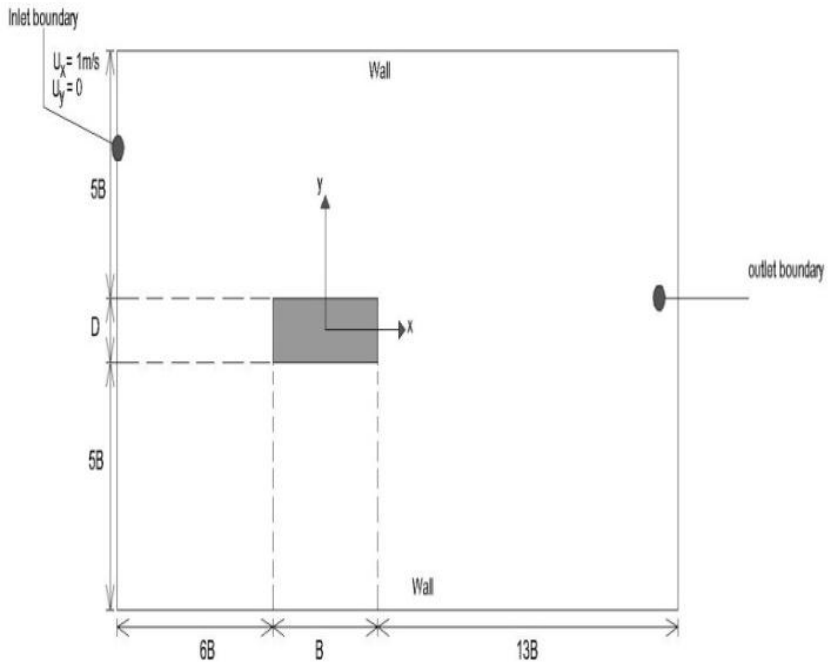


Figure 1: Computational domain (not drawn to scale)

The mesh generation software, Gambit has been used throughout this work to generate the geometry in figure 1 and meshes. Gambit was used to create the computational domain using Top-down approach. The node distributions in all the edges were specified in order to give a better control on the grid distribution. This would be important in order to obtain finer meshes around

the obstacles in the domain and coarse meshes in other regions where there is not much 'action' taking place. The quality of the mesh is inspected based on the equiangle skewness.

$$\text{Equi angle skew} = \max \left[ \frac{\theta_{\max} - \theta_e}{180 - \theta_e}, \frac{\theta_e - \theta_{\min}}{\theta_e} \right] \quad (8)$$

Where;

$\theta_{\max}$  = largest angle in the cell

$\theta_{\min}$  = smallest angle in the cell

$\theta_e$  = angle for equiangular cell

In gambit, the velocity inlet conditions on the velocity field are imposed at the inlet boundaries, the outflow conditions on are imposed at the outlet boundaries. Wall conditions (no-slip conditions) are imposed on both the side surfaces and on the upper-lower surfaces.

For this problem, the model is based on the following assumptions:

- (1) Incompressible fluid
- (2) Newtonian fluid
- (3) Unsteady state
- (4) Laminar flow
- (5) Constant density

### Fluent analysis

The analysis was carried in fluent by importing the meshed file that is generated in gambit. The steps that are followed are given below which include all the conditions and the boundaries values for the problem statement.



- **Checking of mesh and Scaling:** The fluent solver is opened where 2D is selected and then the importing of the meshed file is done. The meshed file then undergoes a checking. Scale is scaled to metres (m). Grid created was changed to metres.
- **Solver and Material Selection and Operating Condition Defining:** The solver is defined first. Solver is taken as pressure based and formulation as implicit, space as 2D and time as unsteady.
- **Material Selection and Operating Condition Defining:** Material selected is air. The properties of air at different Reynolds number are stated in the table 1.

Table 1: Properties of air at different Reynolds numbers

$R_e$	$U$ (m/s)	$D$ (m)	$\rho$ ( $kg/m^3$ )	$\mu$ ( $kg/ms$ )
55	1.0	1.0	1.225	0.0223
75	1.0	1.0	1.225	0.0163
100	1.0	1.0	1.225	0.0123
150	1.0	1.0	1.225	0.0082
250	1.0	1.0	1.225	0.0049
400	1.0	1.0	1.225	0.0031

The Reynolds number is defined as:

$$R_e = \frac{U \times D \times \rho}{\mu} \quad (9)$$

The value of D and U is unity, the density of air is constant but with varied viscosity as stated in table 1.0. The analysis is carried out under operating conditions of 101325 Pascal. Gravity is not taken into consideration.

### ▪ **Boundary Conditions**

**Inlet:** The boundary conditions were already defined in Gambit, but in Fluent it is needed to prompt the velocity and direction at the inlet. Velocity inlet was specified for the inlet boundary and the value of velocity magnitude in the streamline direction is 1m/s.

**Top and bottom walls:** Wall was specified for the sides, top and bottom wall. No slip ( $u = v = 0$ ) boundary conditions were applied to the walls and the walls are stationary.

**Outlet:** The outlet boundary was set as outflow boundary and the flow exit is treated as a zero-normal-gradient outlet boundary with the default value of 1 for flow rate weighting.

The standard discretization method was used for the pressure interpolation scheme and the second order upwind scheme discretization method was used for momentum. Solutions are obtained iteratively using the segregated solver with the Pressure-Implicit with Splitting of Operators (PISO) algorithms to do this.

### ▪ **Initialization**

The initial values of velocity are taken as 1m/s along x direction while that of y is zero. The initial values of velocity were then initialized. Residual monitor and convergence criteria are set up. The convergence criteria of various parameters are listed below.

Continuity - 0.00001

X-Velocity - 0.00001

Y-Velocity - 0.00001

Z-Velocity - 0.00001

The time step size was set to  $\Delta t = 0.025$  and number of iterations is then set up to and iterations starts. The iteration continues till the convergence is reached.

Post-processor used to visualize and quantitatively process the results from the solver. In FLUENT, the analyzed flow phenomena can be presented in vector plots or contour plots to display the trends of velocity, pressure and the plot of the integral flow parameters.

## **Results and discussions**

The cylinder rectangular cross section is characterized by sharp edges and smooth surfaces. A quadrilateral grid is adopted to mesh the area of the computational domain. Quadrilateral meshes would give more accurate solutions, especially if the grid lines are aligned with the flow. The whole computational domain has 19,860 of quadrilateral cells with 20,080 numbers of nodes. The quality of the mesh has been tested in terms of EquiAngle skew. The worst element in the mesh has an EquiAngle skew of 0.03 and skewness should not exceed 0.85. This results show that the quality of the mesh is very good. The adopted structured grid in the x-y plane is depicted in figure 4. Finer meshes were obtained around the obstacles in the domain and coarse meshes in other regions where there is not much ‘action’ taking place.

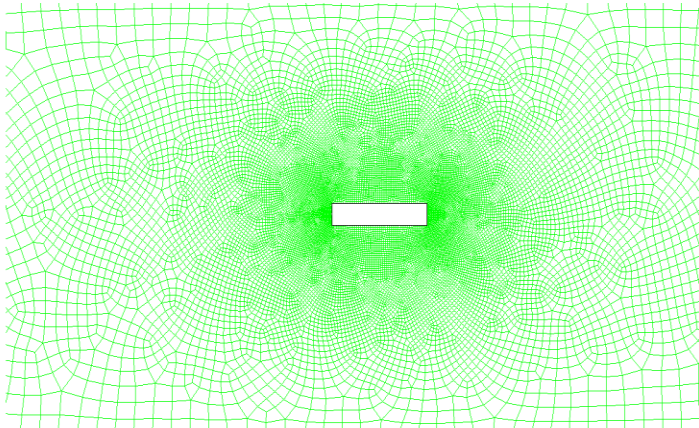


Figure 2: Grid generated around a rectangular cylinder

### **Vortical structure around the rectangular cylinder**

The flow past a rectangular cylinder is deeply affected by the Reynolds number and the cylinder breadth-to-depth ratio. In this Section, we qualitatively describe the sequence of changes that occurs to the flow pattern around a cylinder with  $B/D = 5$  with Reynolds number within the range of 55 and 400. According to Berrone et al, (2010) as  $Re$  is increased, the upstream–downstream symmetry of the streamlines disappears and two eddies appears behind the cylinder. These eddies get bigger with increasing  $Re$ , but do not move off downstream: the flow in the wake is still steady. At sufficiently

high  $Re$ , the flow becomes unsteady due to wake instability mechanisms and the phenomenon of vortex shedding, known as von Kármán Street, develops. Figure 3a shows the Instantaneous vorticity contour computed at Reynolds numbers between 55 and 75; which that indicate a steady configuration consisting of two symmetric vortices in the cylinder wake. At Reynolds numbers of 100 to 225, the flow field is steady and two nearly symmetrical vortices are developed behind the cylinder as shown in figure 3b. At Reynolds numbers 100 to 225, the flow in the wake is still steady but instability occurs and vortex shedding appears and flow becomes unsteady at Reynolds numbers 250 to 400 as shown in figure 3c.

When the flow regime is steady, the final flow configuration obtained by the FLUENT code does not depend on time and the time step- length is progressively enlarged during the transitory process that leads to final stationary flow.

Figure 4 shows the velocity contours for laminar flow around a rectangular cylinder. This shows the magnitude of the velocity across the section of the rectangular cylinder. On the side of the bluff body where the vortex is being formed, the fluid velocity is higher and the pressure is low. The blue region is the minimum velocity across the cylinder wake which is close to the rectangular cylinder whereas the maximum velocity (red region) is far away from the cylinder wake.

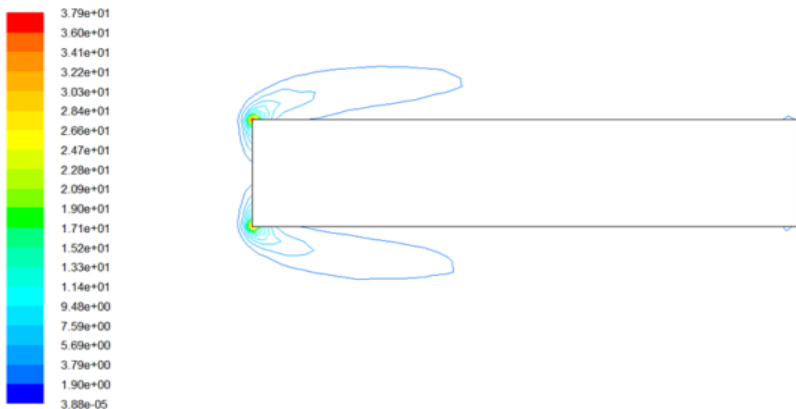


Figure 3a: Instantaneous vorticity contour around the rectangular cylinder for  $Re$ : 55 to 75.

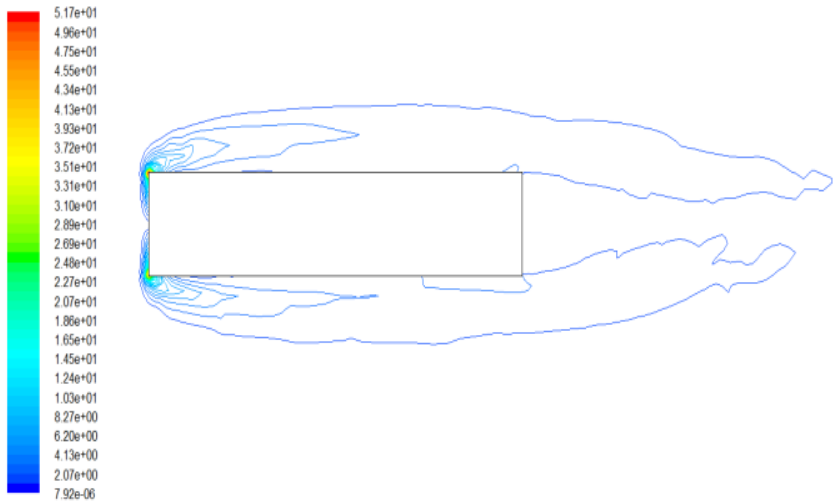


Figure 3b: Instantaneous vorticity contour around the rectangular cylinder for Re: 100 to 225.

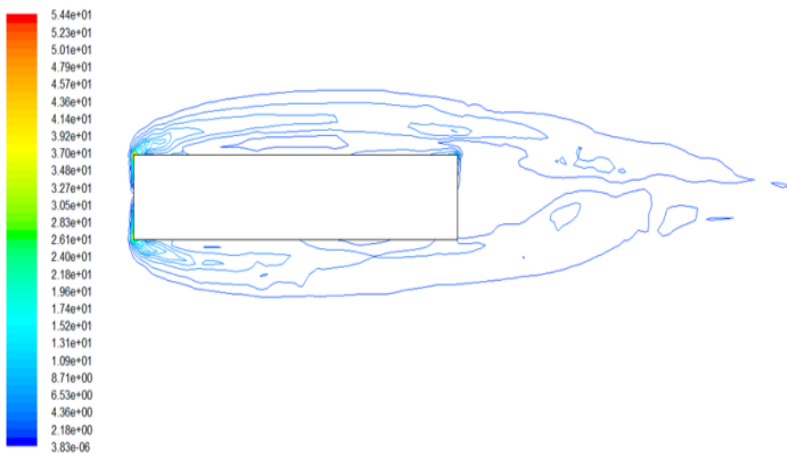


Figure 3c: Instantaneous vorticity contour around the rectangular cylinder for Re: 225 to 400

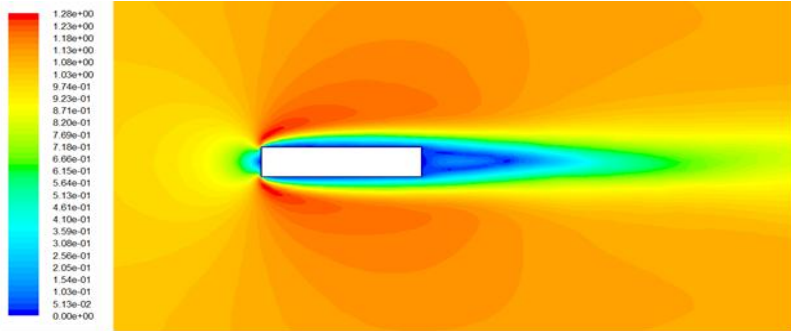
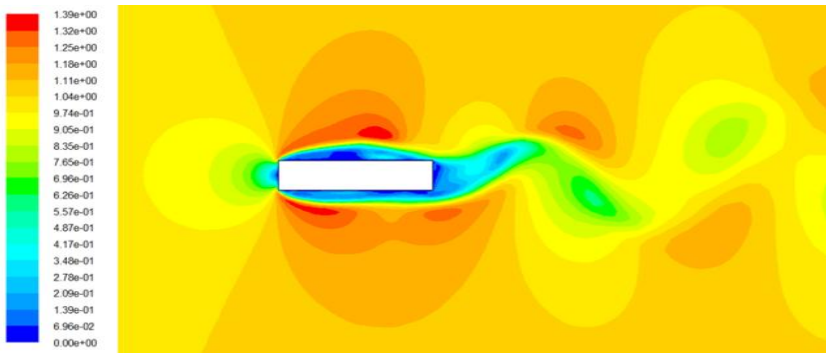
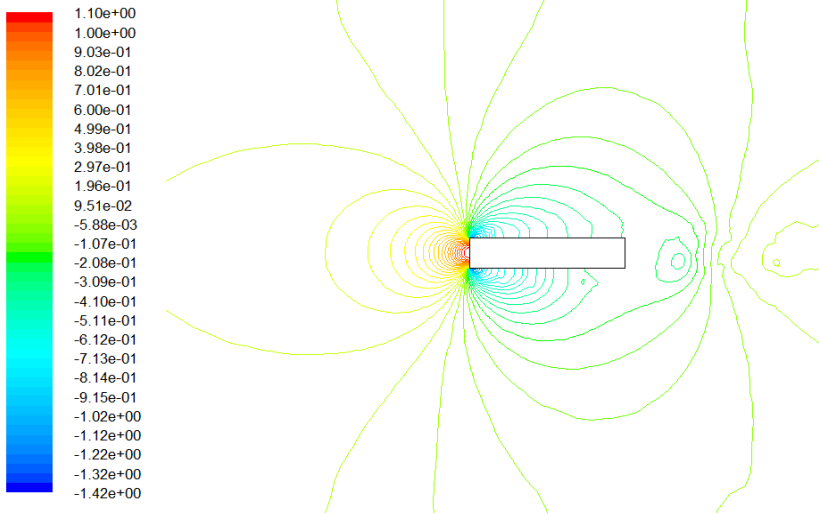
(a)  $Re = 55$ (b)  $Re = 400$ 

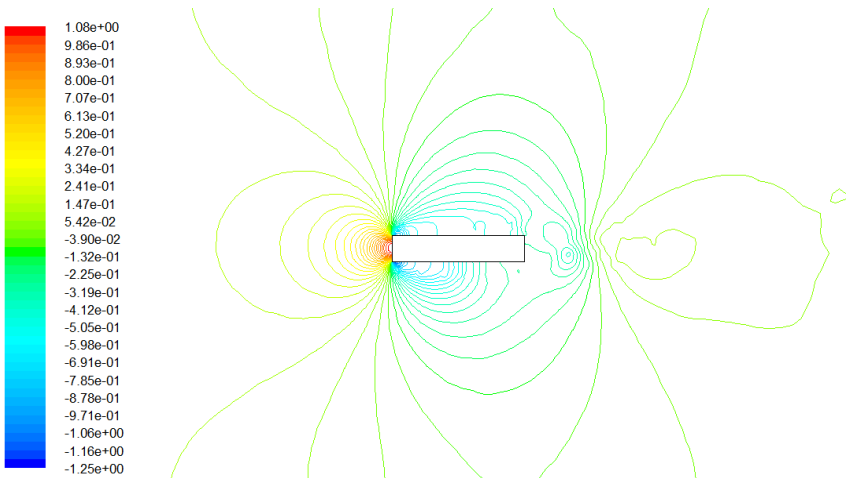
Figure 4: Velocity contours for laminar flow around a rectangular cylinder

### Pressure distribution around the rectangular cylinder

The pressure coefficient is a dimensionless parameter which describes the relative pressure throughout the flow field. Instantaneous pressure contours are plotted in figure 5 for the laminar flows around a rectangular cylinder. On the side of the bluff body where the vortex is being formed, the pressure is low. The pressure coefficients at the centreline of the obstacles are plotted in figure 6. The vortex street is obvious from these contours and plots, with staggered low-pressure centres at the core of vortices. It should also be noted that these pressure contour at the leading edge is high but the pressure coefficient is relative low at the centre of the obstacle.

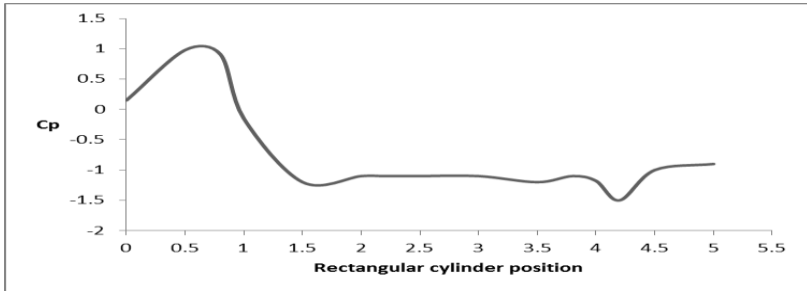


(a)  $Re = 55$

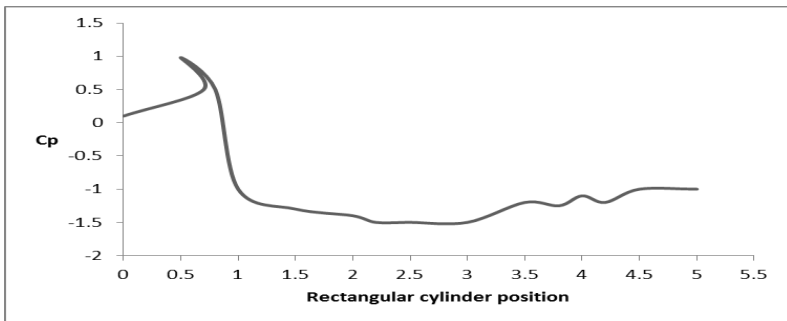


(b)  $Re = 250$

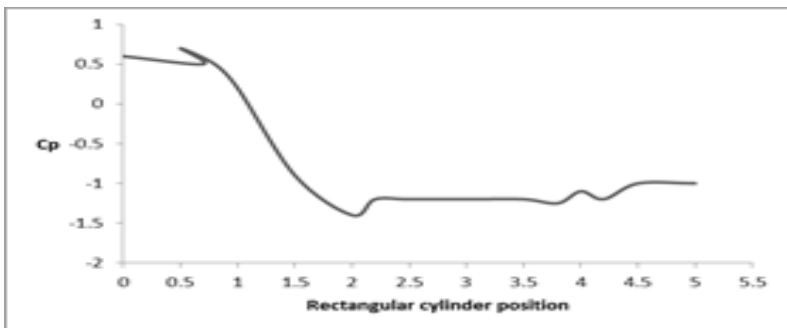
Figure 5: Pressure distribution contours for laminar flow in a rectangular cylinder.



(a)  $Re = 55$

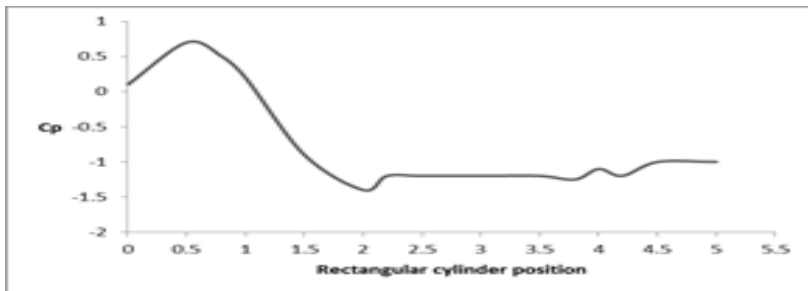


(b)  $Re = 75$

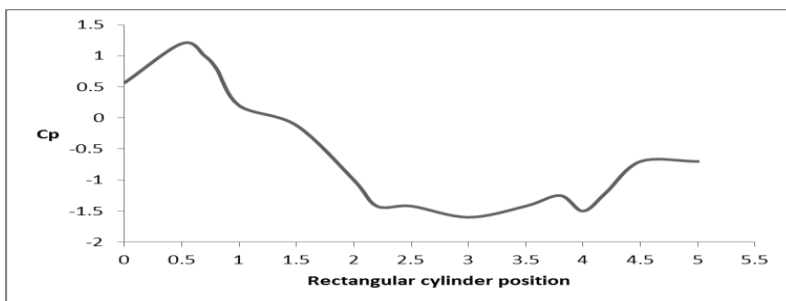


(c)  $Re = 100$

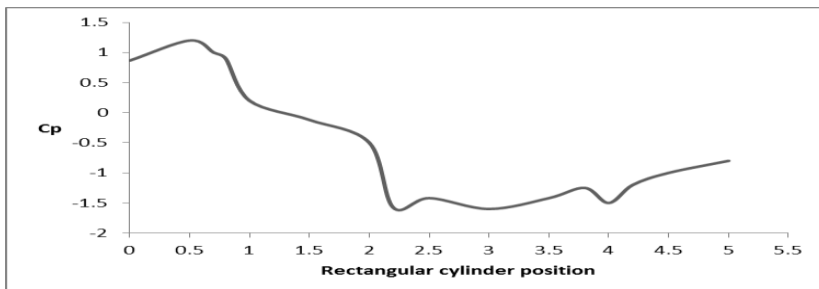




(d)  $Re = 150$



(e)  $Re = 250$



(f)  $Re = 400$

Figure 6. Pressure coefficient at the centerline of the rectangular cylinder

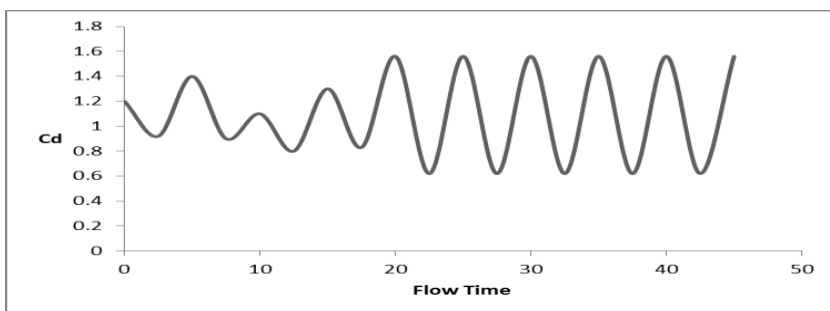
### Integral flow parameters

The main aerodynamic integral parameters (Strouhal number, lift and drag coefficient) are analyzed in this section. The unsteadiness occurs where a bluff body obstructs the free flow motion. The significant separation areas generated are the main source of drag forces. The time is non-dimensionalised by  $U$  and  $D$ . The non-dimensional time-step is set equal to 0.025, which provides an accurate advancement in time. The simulation is extended to 200 non-dimensional time units in order to have a long enough statistical sample to obtain converged statistics, after having excluded the initial transient.

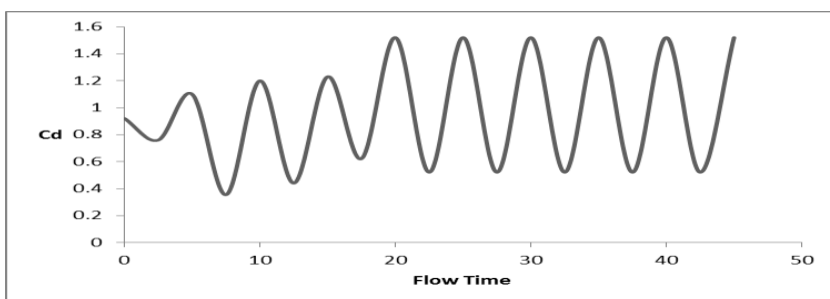
Figure 7 and 8 shows the periodic behaviour of the drag and lift coefficients respectively, which fluctuate in a fairly sinusoidal way over a period of time. FLUENT computed the drag coefficient, lift coefficient and strouhal number. Investigation was carried out for Reynolds numbers of 55, 75, 100, 150, 250 and 400. Strouhal Number ( $St$ ), total drag coefficient ( $C_D$ ), pressure drag coefficient ( $C_{dp}$ ), lift coefficient ( $C_L$ ) and pressure coefficients at the centreline ( $C_{pc}$ ) were determined from numerical calculation. The results at various Reynolds number are given in Table 2. Pressure drag is drag due to the integrated surface pressure distribution over the body. The flow around the rectangular cylinder separates, resulting in a region of high surface pressure on the front side and low surface pressure on the rear side and thus significant pressure drag. The total drag force is the combination of drag due to pressure and drag due viscous effect. The viscous drag is due to the friction between the fluid and the surfaces over which it is flowing while pressure drag comes from the eddying motions that are set up in the fluid as it flows through the bluff body. The forces caused by vortex shedding phenomenon must be taken into account when designing structures in form of rectangular cylinder. Figure 9 shows that Strouhal numbers are function of the Reynolds number. The Strouhal number can be strongly affected by the Reynold number. Concretely, the Strouhal number seems to gradually increase with the increase of Reynold number. Figure 10 indicates the effect of lift and drag coefficient as function of the Reynolds number.

Table 2: Effect of Reynolds number

Re	St	$C_D$	$C_{DP}$	$C_L$	$-C_{Pc}$
55	0.102	1.565	1.446	0.067	0.841
75	0.122	1.524	1.455	0.101	0.936
100	0.129	1.461	1.439	0.157	1.055
125	0.136	1.423	1.412	0.212	1.132
250	0.139	1.526	1.579	0.404	1.288
400	0.158	1.545	1.602	0.537	1.356



(a)  $Re = 55$



(b)  $Re = 75$

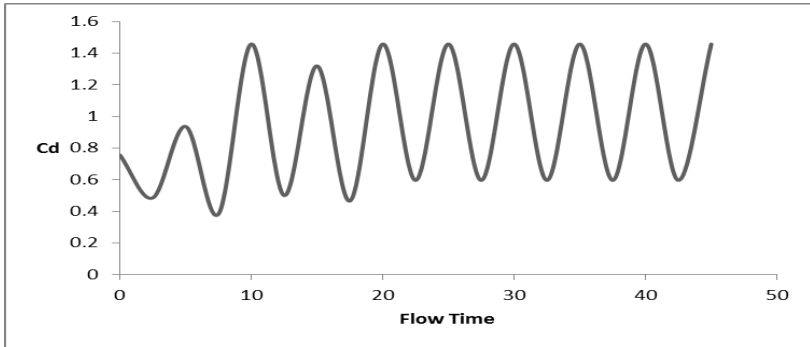
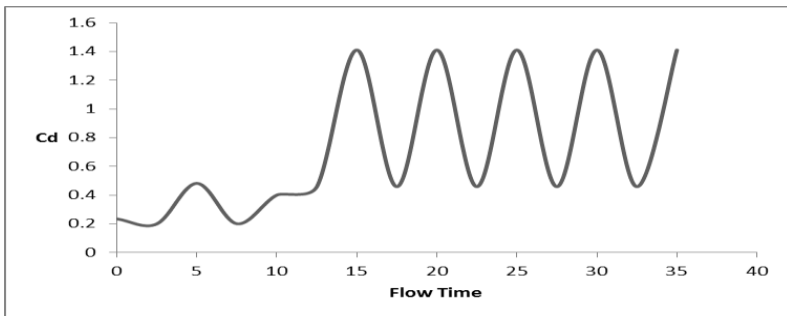
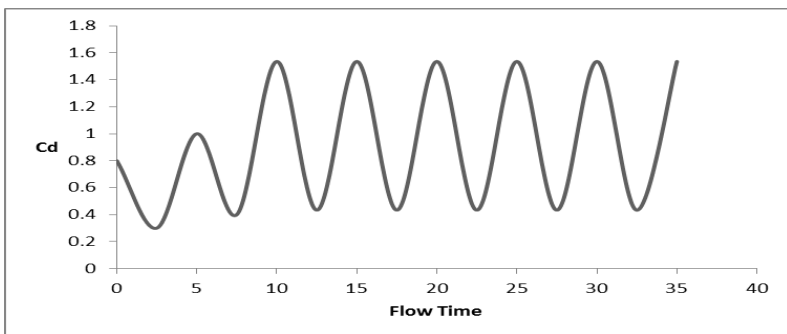
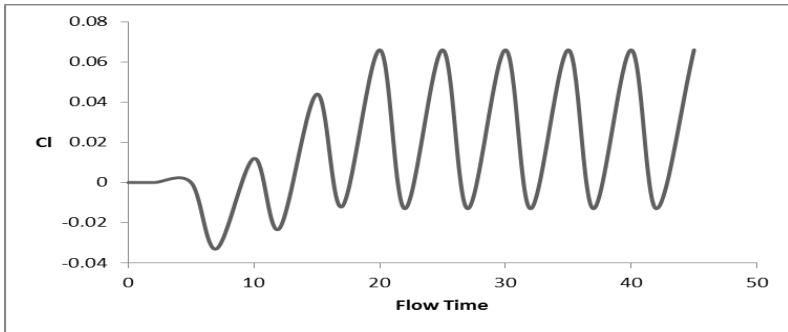
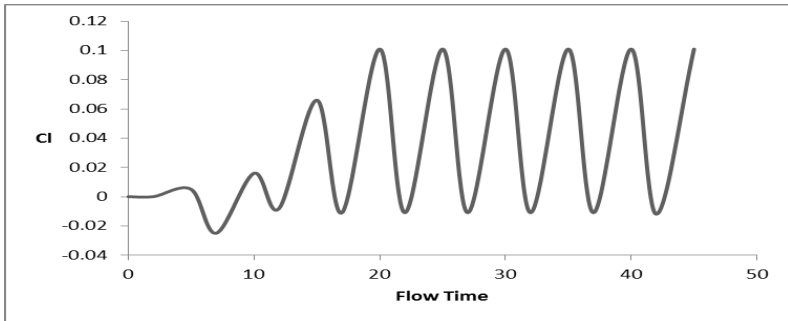
(a)  $Re = 100$ (b)  $Re = 125$ 

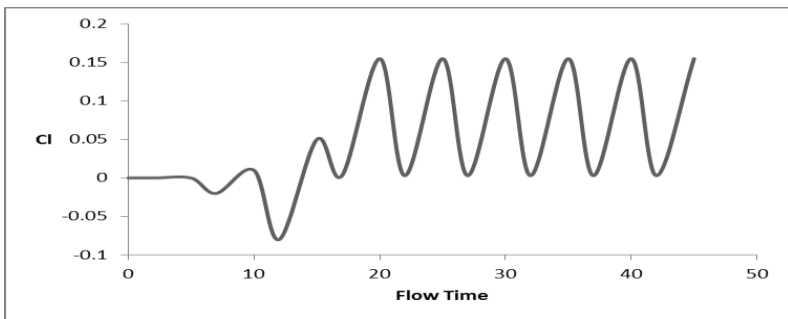
Figure 7. The time histories of the drag coefficients



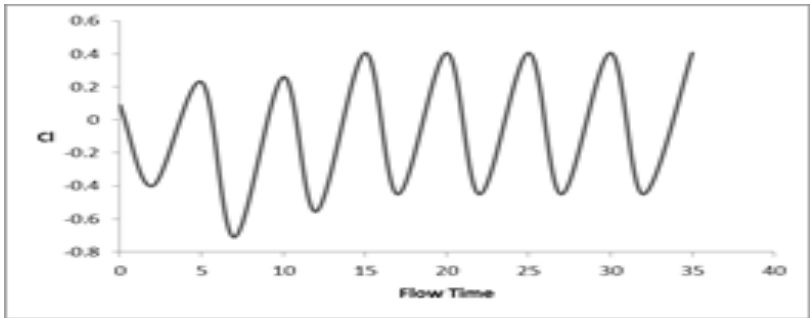
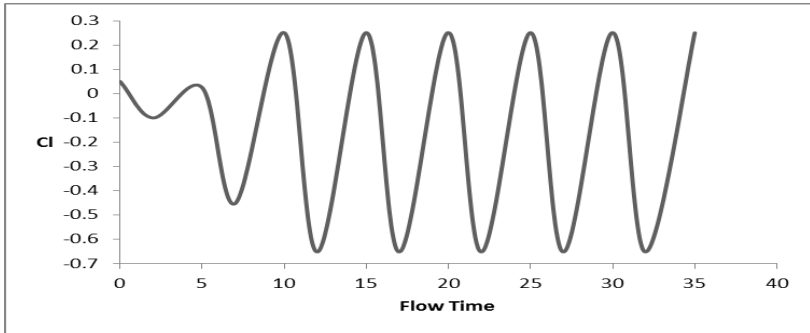
(a)  $Re = 55$



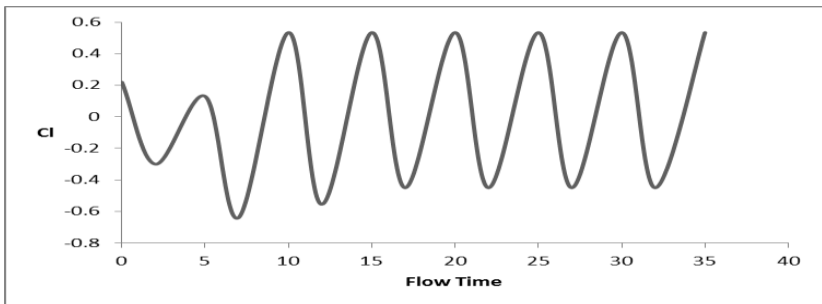
(b)  $Re = 75$



$Re = 100$



(e)  $Re = 250$



$Re = 400$

Figure 8. The time histories of the lift coefficients

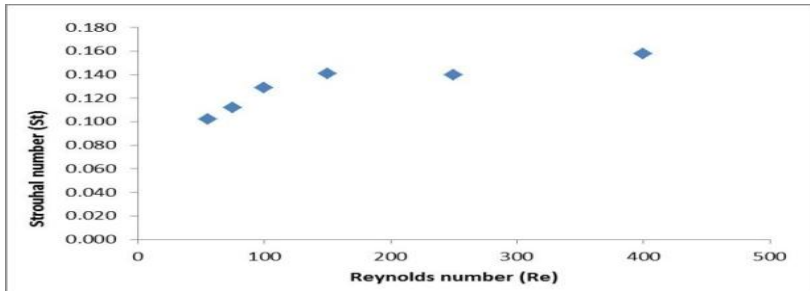


Figure 9. Variation of strouhal number against Reynolds number

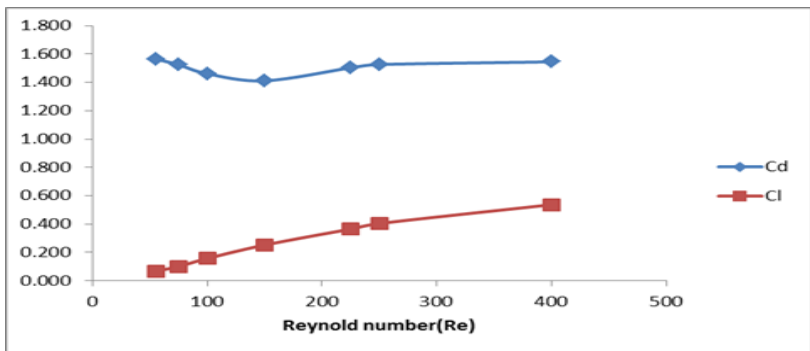


Figure 10: Variation of lift and drag coefficient against Reynolds number

### Conclusion

A computational study has been proposed in this work to analyse some flow features at low Reynolds numbers (laminar flow) around a fixed rectangular cylinder with chord-to-depth ratio equal to 5. Gambit has been used throughout this work to generate the geometry and meshes. Gambit is used to create the computational domain using Top-down approach and the computational fluid dynamics analysis is done using fluent software. Fluent used control volume method to discretize the 2D incompressible Navier Stokes equation. This CFD software solves the equations of mass and momentum in each control volume, guarantying conservation for each variable.

Flow parameters such as drag and lift coefficient, Strouhal number, vorticity, pressure and velocity contours are investigated in this paper. Strouhal

number, lift and drag coefficient obtained for rectangular cylinder were reported in the thesis. The Instantaneous vorticity contour computed at Reynolds numbers between 55 and 75 indicate that a steady configuration consisting of two symmetric vortices in the cylinder wake. At Reynolds numbers of 100 to 225, the flow field is steady and two nearly symmetrical vortices are developed behind the cylinder. At Reynolds numbers 100 to 225, the flow in the wake is still steady but instability occurs and vortex shedding appears and flow becomes unsteady at Reynolds numbers 250 to 400. Staggered low-pressure is centered at the core of vortices and it should also be noted that these pressure contours at the leading edge is high. The forces caused by vortex shedding phenomenon must be taken into account when designing structures in form of rectangular cylinder.

It is recommended that further studies are required to check the present proposal, to complete the knowledge of the main fluid flow phenomena which drive the section aerodynamics and to provide a complete database for validation and comparison purposes. In this perspective, the benchmark could offer a useful research framework to the scientific community adopting both computational and experimental approaches.



## References

- Ahmed, S.R. (1998).. Computational Fluid Dynamics, Chapter XV in Hucho, W.H (Ed.), *Aerodynamics of Road Vehicles*. 4th Edition, Warrendale, PA, USA: SAE International.
- Almeida, O., S. S. Mansur, A. Silveira-Neto (2008). On the flow past rectangular cylinders: physical aspects and numerical simulation. *Engenharia Térmica (Thermal Engineering)*, Vol. 7, No 01, p. 55-64.
- Behr, M.; Hastretier, D.; Mittal, S.; and Tezduyar, T. E. (1995). Incompressible Flow past a circular cylinder: dependence of the computed flow field on the location of the lateral boundaries, *Comput. Meth. Appl. Mech. Engg.*, vol (123), 309-316.
- Berrone S, V. Garbero, M. Marro (2011). Numerical simulation of low-Reynolds number flows past rectangular cylinders based on adaptive finite element and finite volume methods, *Computers & Fluids* 40 92–112.
- Bruno L, Fransos D, Coste N, Bosco A. (2008). 3D flow around a rectangular cylinder: a computational study. *Journal of Wind Engineering and Industrial Aerodynamics*, 98 (2010) 263–276.
- Charles Meneveau (2010).Turbulence: Subgrid-Scale Modeling, *Johns Hopkins University Scholarpedia*, 5(1):9489.
- Fluent – Commercially available CFD software package based on the Finite Volume method. Fluent tutorial guide (2006).
- Mustafa Sarioglu, Tahir Yavuz (2000). Vortex Shedding From Circular and Rectangular Cylinders Placed Horizontally in a Turbulent Flow. *Turk J Engin Environ Sci* 24, 217-228.
- Nakaguchi H, Hashimoto K, Muto (1968). An experimental study on aerodynamics drag of rectangular cylinders. *J. Japan Society of Aeronautical and Space Sci.*, Vol.16, p. 1-5.

- Norberto Nigro, German Filippini, Gerardo Franck, Mario Storti and Jorge D'Elia (2005). Flow around a sharp-edged surface-mounted cube by large eddy simulation. *In Mecánica Computacional*, vol. XXIV.
- Okajima A. (1990). Numerical simulation of flow around rectangular cylinders. *Journal of Wind Engineering and Industrial Aerodynamics*, vol 33, 171-180.
- Okajima A. (1982). Strouhal number of rectangular cylinders. *Journal of Fluid Mechanics*, Vol.123, p. 379-398.
- Rodney C., Thomas M., Paul E., Thomas E., Mark A., Alan R., and Scott Wunsch (2002). On the Development of the Large Eddy Simulation Approach for Modeling Turbulent Flow: *LDRD Final Report*.
- Rokugou A, Okajima A , Kamiyama K. (2002). Numerical Analysis of Flow around Rectangular Cylinders with Various Side Ratios. *Japan Society of Mechanical Engineers* vol.68; no.670; page.1608-1613.
- Sohankar, A., Norberg, C.; and Davidson, L. (1998). Low-Reynolds-Number Flow around a Square Cylinder at Incidence: Study of Blockage, Onset of Vortex Shedding and Outlet Boundary Condition, *International Journal for Numerical Methods in Fluids* vol (26), pp 39-56.
- Yu Dahai, Ahsan Kareem (1998). Parametric study of flow around rectangular prisms using LES. *Journal of Wind Engineering and Industrial Aerodynamics* 77&78 p. 653-662